

DESIGN STUDY OF 50 kG/in. QUADRUPOLE MAGNET

Kenji Ishibashi and A.D.McInturff

September 1982

A design study was made on a three-shell quadrupole magnet with an operational field gradient of 2.0 T/cm, which would represent one of the world's highest values for an accelerator quadrupole. The conductor specifications required the magnet to be cooled by 1.8K, 1 atm superfluid helium. Magnetic and mechanical considerations are described and discussed.

INTRODUCTION

Since the proposition of pressurized superhelium refrigeration by the Saclay-Grenoble group,¹ attempts have been initiated in some laboratories to apply it to 10.0T accelerator dipole magnets.² As is well known, the requirements for fabrication of a quadrupole magnet of a given strength are less severe than those of a dipole, in order to achieve the same high current density efficiency of the superconductor used. Therefore, a quadrupole magnet may provide a suitable check of superconductor performance and feasibility of a superfluid-(He) cooled high field magnet system. A design study was made and parameters were obtained for a quadrupole magnet design which utilizes a ternary alloy conductor cooled by 1.8K pressurized superfluid helium. This design has an operational field gradient of 2.0 T/cm. This field gradient is more than twice that of the present Energy Saver quadrupole magnets, and is attained by a three-shell winding structure and cold iron. The design requires a three-inch diameter aperture. The peak field in winding is 10.0T for 2 T/cm.

MAGNET PARAMETERS

Specifications of conductor for the quadrupole magnet are listed in Table I. Although it depends on critical current density achieved in research and development of the superconductor, the number of strands in a cable was chosen as 25, assuming the critical current density of superconductor of 155 kA/cm² at 11.0T, 1.8K. The cable

insulation consists of two overlapping spiral layers of Kapton, .001" and .002" thick, with each having 20% gap. The resulting winding modulus is 3 Mpsi at room temperature and 6 Mpsi at 77K and below. Figure 1 shows critical current density of the superconductor, and current density necessary for the field gradient of 2.0 T/cm. Current density for 23 and 21 strand cables is also indicated for comparison. A dashed line in the Figure represents data obtained from one of the best binary alloys ever reported.³

Magnet parameters are listed in Table II, and the cross sectional view is shown in Figure 2. Laminated iron plates (iron collars) are kept cold and used to enhance the field gradient to as high as possible. The outer stainless steel ring shown in Figure 2 has two purposes. The first function is to compensate for the comparatively low thermal contraction of iron collars. The ring therefore maintains the room temperature preload on the winding during cooldown and at liquid helium temperature. The second purpose of the stainless ring is to reduce stress concentration in the brittle iron collar during magnet excitation. The large iron keys also serve this purpose.

Because of the close proximity of the iron collars to the windings, this magnet design has a substantial flux saturation effect on its transfer function and harmonics. The transfer function at $I = 5.6$ kA is 16% less than that at field below the iron saturation.

Field harmonics are summarized in Table III for two kinds of magnetic length (90.55 and 131.89"). The sensitivity of the harmonics to the winding accuracy is shown in Figures 3 and 4. Those displacement effects on harmonics were calculated for simplicity for two constant iron permeabilities, one, infinite (solid line) and another, unity (dashed line). Figure 3 shows that the iron desensitizes the radial winding displacement effect on harmonics due to the mirroring of the current block in it. Figures 3 and 4 indicate that the present three-shell quadrupole magnet has similar harmonic sensitivity as that of the present Energy Saver quadrupole magnet.

The magnet end winding is shown in Figure 5, where cross sectional view along the magnet axis is drawn on a plane of $\theta = 45^\circ$ in (a). Magnetic field without iron was calculated by GFUN, and is shown in (b) for the points indicated by dots in this Figure. The peak field on the plane is 69 kG. End field computation of the alternate configuration is given in Reference 4. Although the magnet end is designed to lie outside of the iron collars, there is a slight field enhancement due to the iron, as shown in Figure 6. The field enhancement shown in the Figure is 1 kG, and the total field is therefore 70 kG.

MECHANICAL CONSIDERATION

Magnetic pressure on the winding is shown in Figure 7 for a field gradient of 2 T/cm. The highest pressure on the median plane is 7.8 kpsi, and 30% higher⁴ than that of the Energy Saver dipole magnet at a central field of 43 kG.

Deflection of the magnet winding is shown in Figure 8, as predicted by a simple two-dimensional calculation. The iron collars were assumed to have no laminar structure, and be infinitely long along the magnet axis. Preload on the winding was not applied in this computation. Dashed lines stand for the original form, and solid lines for the deflected one. As indicated in the Figure, the maximum winding displacement in the azimuthal direction is 1.6×10^{-3} in. The radial displacement of iron on the median plane is as low as 0.4×10^{-3} in. This radial displacement is underestimated because the laminated structure is neglected.

Since the iron collar lamination thickness, .060 in., is thin compared to their width, it may be regarded as a membrane. The collar structure was therefore calculated three-dimensionally as shown in Figure 9. Only two pieces were considered in the "z" direction (magnet axis), and were imposed as a periodic boundary condition along "z", therefore, part of an infinitely laminated structure. Utilizing the quadrupole symmetry present, only the first octant was considered for calculation.

The magnetic force was applied on the collar's inner surface. This resulted in the displacements shown in Figure 8 being predicted by the two-dimensional calculation.

The resultant displacements are shown in Figure 10 for a field gradient of 2 T/cm. Preload⁵ corresponding to the radial magnetic force at 2 T/cm was assumed in the calculation. The displacement of the iron collars on the median plane due to this preload is 1.6×10^{-3} in. Although this value is larger than that in Figure 8, it is still lower than the 3 to 4×10^{-3} in. observed in the Energy Saver dipole magnets.

Contour lines of effective stress⁶ are plotted in units of kpsi in Figure 11. The peak stress in the iron collar is 10.6 kpsi. The stainless steel ring and the comparatively large iron key prevent the stresses from concentrating around the key groove in the iron collar.

Properties of low carbon steel at liquid helium temperature⁷ are listed in Table IV. Small values of Charpy impact strength and elongation before failure are indications that the iron is brittle at low temperature. The peak operating stress of 10.6 kpsi on the collar is much lower than values of yield stress and fatigue strength given in the Table of ultimate properties (Table IV).

CONCLUSION

Design parameters were obtained for the 1.8K helium-cooled 2 T/cm quadrupole magnet that seem to be reasonable. The magnet seems to be state-of-the-art Engineering and technically possible at the present time. The only parameter which has not been demonstrated to date is the current density at field of 11T and 1.8K. The design (with proper safety factors) requires 155 kA/cm^2 while the best so far obtained is 130 kA/cm^2 , or 20% increase is needed.

REFERENCES

1. For example: J.L.Augueres, R.Aymar, G.BonMardion, G.Claudet, G.Faure Brac, J.Plancoulaine and L.Senet, Cryogenics 20, 529 (1980).
2. C.Taylor, R.Meuser, S.Caspi, W.Gilbert, W.Hassenzahl, C.Peters and R.Wolgast, "High-Field Superconducting Accelerator Magnets", Presented at the Ninth International Cryogenic Engineering Conference, Kobe, Japan, May 1982; also LBL-14400.
3. H.Hirabayashi, "8-10T Dipole Magnets at KEK", Presented at the ICFC Workshop on Possibilities and Limitations of Superconducting Magnets for Accelerators, Serpukhov, USSR, October 1981.
4. K.Ishibashi and A.D.McInturff, Fermilab Internal Report TM-1132, September 1982.
5. K.Ishibashi and A.D.McInturff, Fermilab Internal Report TM-1065, August 1981.
6. K.Ishibashi and A.D.McInturff, "Stress Analysis of Superconducting 10T Magnets for Synchrotron", Presented at the Ninth International Cryogenic Engineering Conference, Kobe, Japan, May 1982.
7. R.Barron, Cryogenic Systems, McGraw-Hill Book Company, New York (1966).

TABLE I
CONDUCTOR

<u>Strand</u>	
Superconductor type	NbTiTa
Critical current density	155 kA/cm ² at 11T, 1.8K
Filament diameter	8 μm
Copper/superconductor volume	1.5
Diameter	0.0268"
<u>Cable</u>	
Number of strands	25
Nominal dimensions (including insulator)	0.338×0.0548"

TABLE II
QUADRUPOLE MAGNET PARAMETERS

Number of shells	3
Coil inner diameter	3"
Number of layers:	
1st shell	10 4
2nd shell	21
3rd shell	25
Azimuthal angle:	
1st shell	18.97° 24.50 - 32.03°
2nd shell	32.67°
3rd shell	33.05°
Current/turn for 50 kG/in	5.6 kA
Inductance/length	14.4 mH/m
Iron - inner diameter	5.14"
outer diameter	13.0"

TABLE III

HARMONICS

	<u>Magnetic Length</u>	
	85.55"	126.89"
<u>Straight Section</u>		
At low current		
Transf. func.	10.471 kG/in./kA	10.466 kG/in./kA
12 p	$-7.12 \times 10^{-4} \text{ in.}^{-4}$	$-7.79 \times 10^{-4} \text{ in.}^{-4}$
20 p	$-0.66 \times 10^{-4} \text{ in.}^{-8}$	$-0.68 \times 10^{-4} \text{ in.}^{-8}$
28 p	$0.45 \times 10^{-4} \text{ in.}^{-12}$	$0.45 \times 10^{-4} \text{ in.}^{-12}$
36 p	$-0.33 \times 10^{-4} \text{ in.}^{-16}$	$-0.33 \times 10^{-4} \text{ in.}^{-16}$
5.55 kA		
4 p	50.027 kG/in.	49.996 kG/in.
12 p	$2.40 \times 10^{-4} \text{ in.}^{-4}$	$1.62 \times 10^{-4} \text{ in.}^{-4}$
20 p	$0.25 \times 10^{-4} \text{ in.}^{-8}$	$0.23 \times 10^{-4} \text{ in.}^{-8}$
28 p	$-0.45 \times 10^{-4} \text{ in.}^{-12}$	$-0.45 \times 10^{-4} \text{ in.}^{-12}$
36 p	$0.45 \times 10^{-4} \text{ in.}^{-16}$	$0.45 \times 10^{-4} \text{ in.}^{-16}$
<u>Magnet End (No iron yoke)</u>		
Field Integral at 5.55 kA		
4 p	250.3	kG
12 p	-1.03	kG/in. ⁴
20 p	-1.28×10^{-1}	kG/in. ⁸
28 p	-3.61×10^{-3}	kG/in. ¹²
36 p	-8.70×10^{-3}	kG/in. ¹⁶
<u>Total</u>		
Field Integral at 5.55 kA		
4 p	4529.96 kG	6693.99 kG
12 p	0	0
20 p	$-0.05 \times 10^{-4} \text{ in.}^{-8}$	$0.03 \times 10^{-4} \text{ in.}^{-8}$
28 p	$-0.46 \times 10^{-4} \text{ in.}^{-12}$	$-0.46 \times 10^{-4} \text{ in.}^{-12}$
36 p	$0.43 \times 10^{-4} \text{ in.}^{-16}$	$0.44 \times 10^{-4} \text{ in.}^{-16}$
<u>Stored Energy</u>	509 kJ	742 kJ
<u>Inductance</u>	33.1 mH	48.2 mH

TABLE IV

PROPERTIES OF LOW CARBON STEEL AT 4.2K

Low Carbon Steel	AISI C1020 (0.2% C, 0.9% Mn, 0.04% S)
Ultimate stress	140 kpsi
Yield stress	100 kpsi
Fatigue strength	105 kpsi (10^6 cycle)
Charpy impact strength	5 ft-lb
Elongation before failure	5%
Elastic modulus	32 Mpsi

Current density
(kA/cm²)

J_c : Critical current density
Marks (circle, triangle and square):
Current density and peak field
in the windings for 50 kG/in

Copper/superconductor = 1.5 (volume)

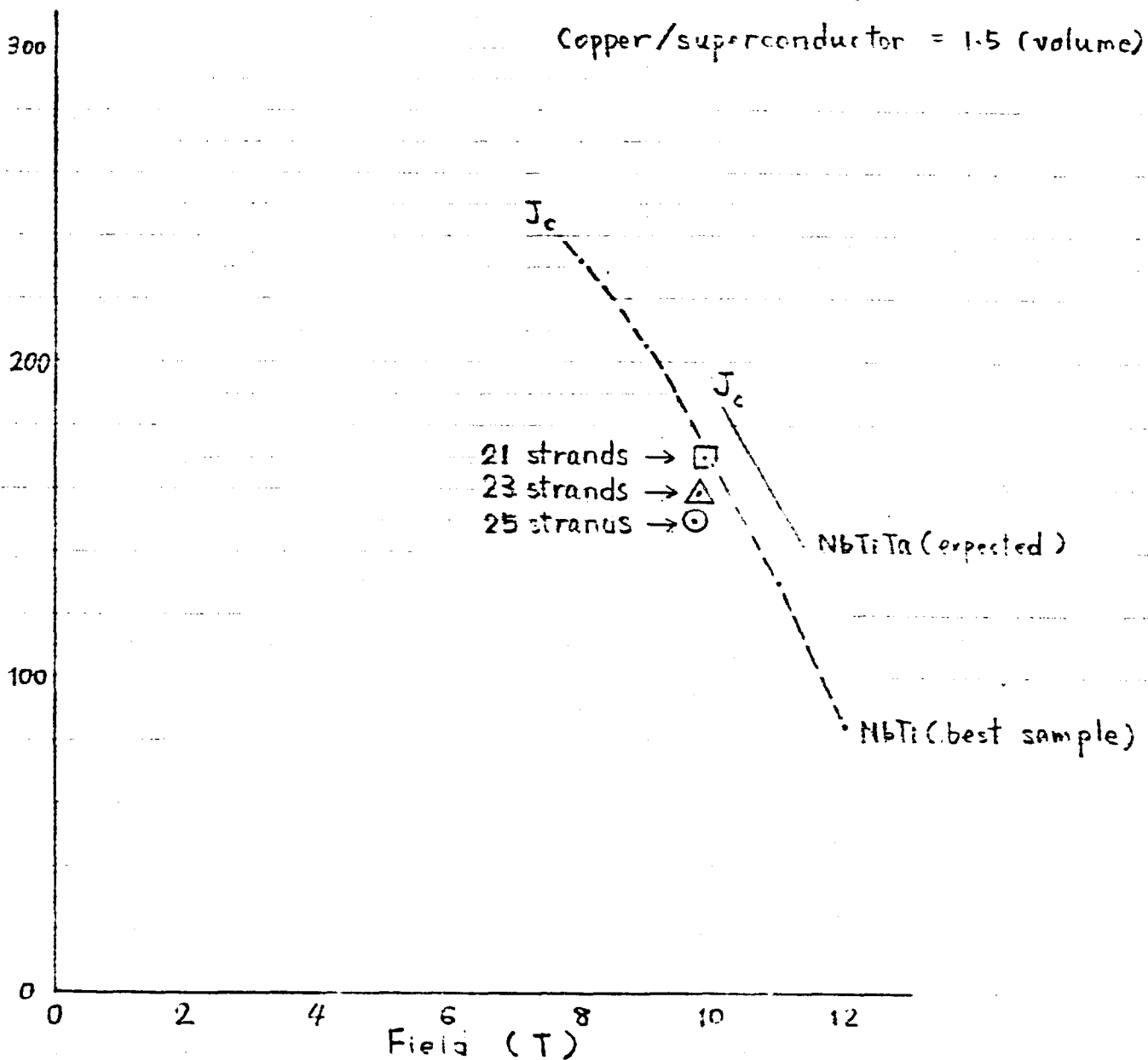


Figure 1. Current density of superconductor at 1.8 K

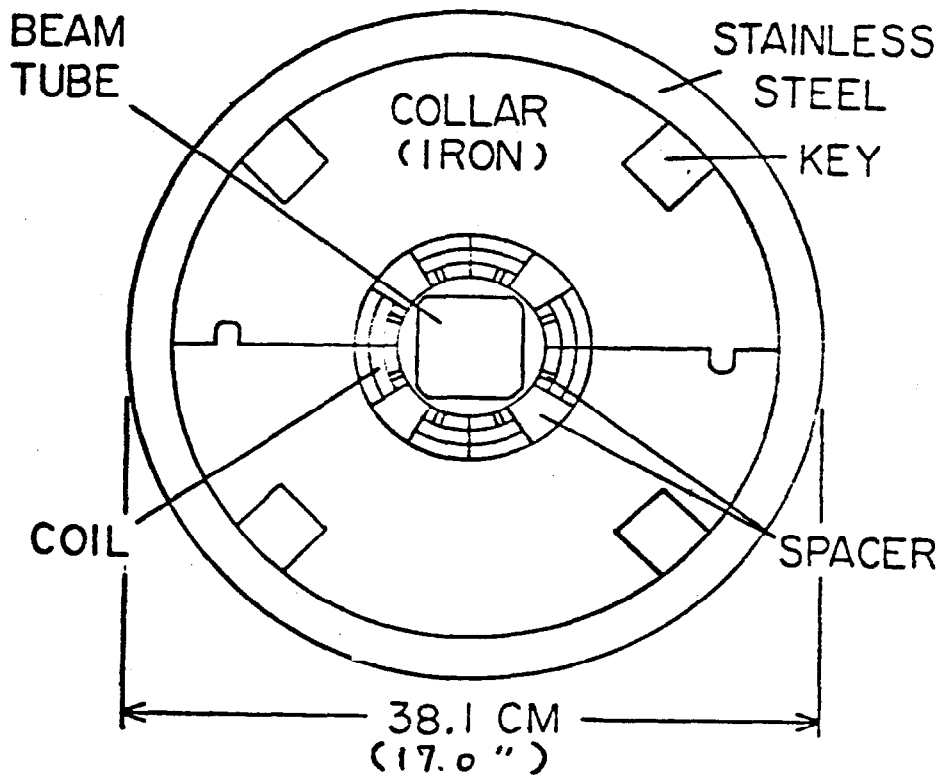
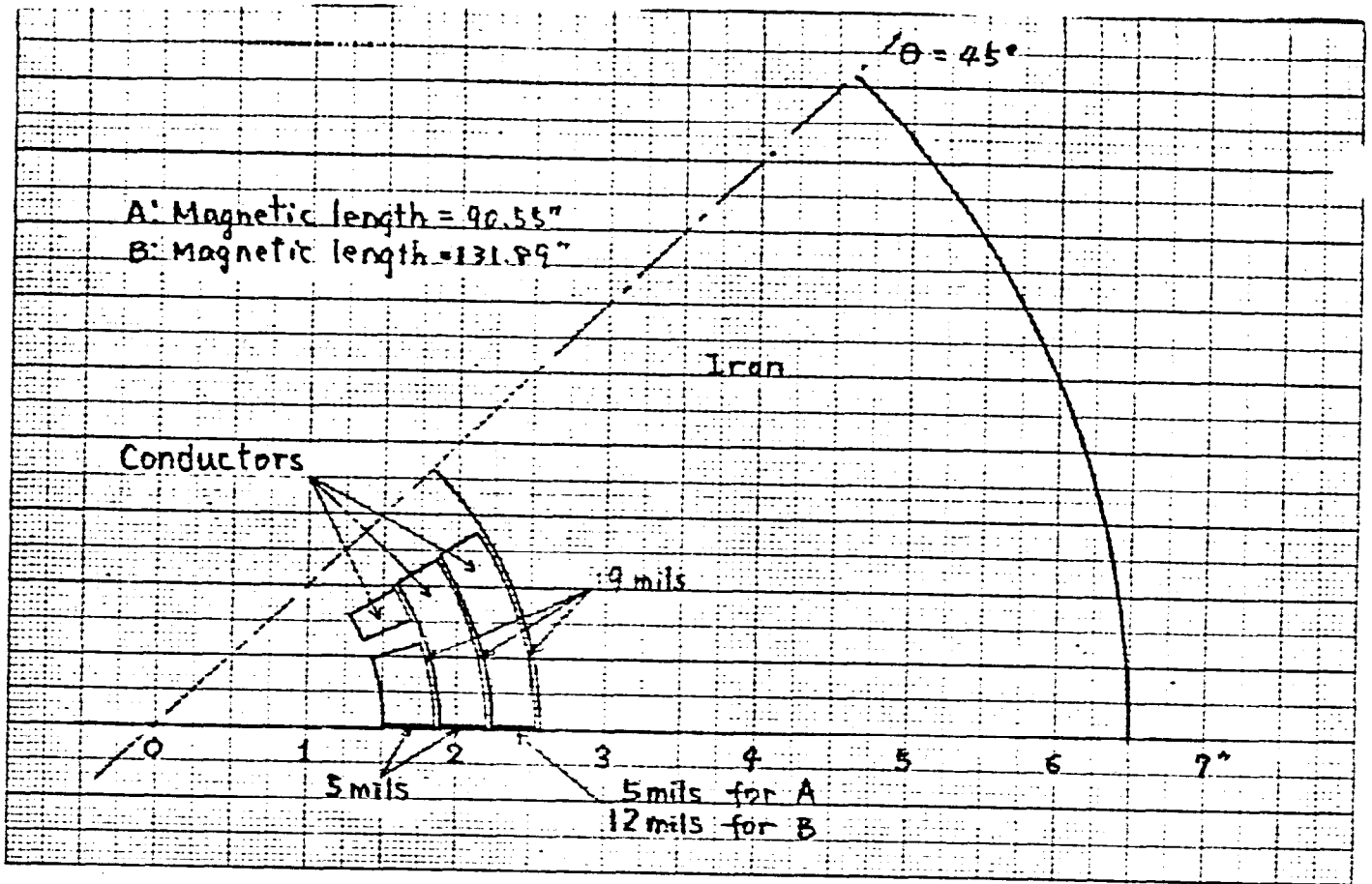


Figure 2 Cross sectional view of the quadrupole magnet

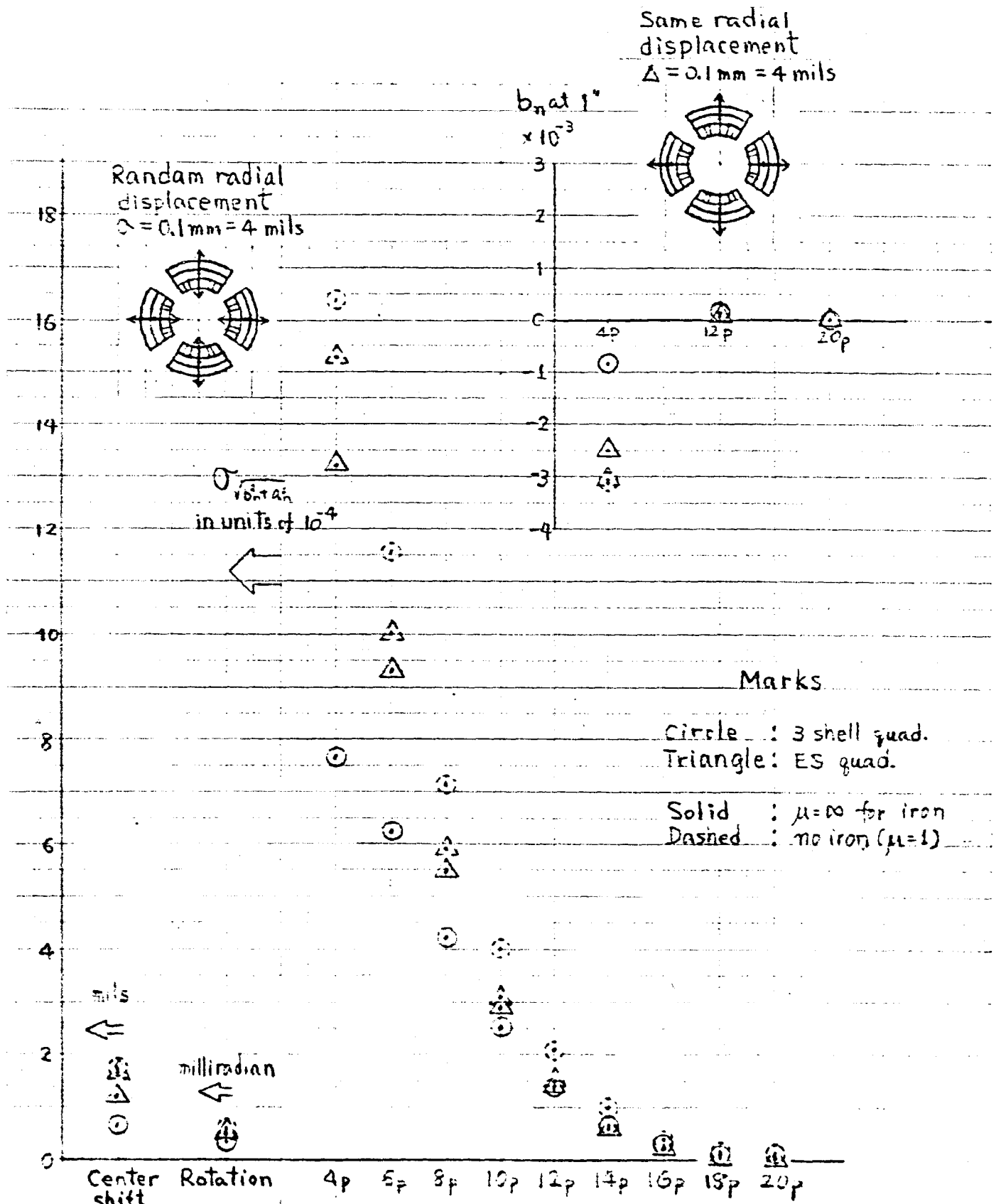


Figure 3 Harmonics variation for radial displacement

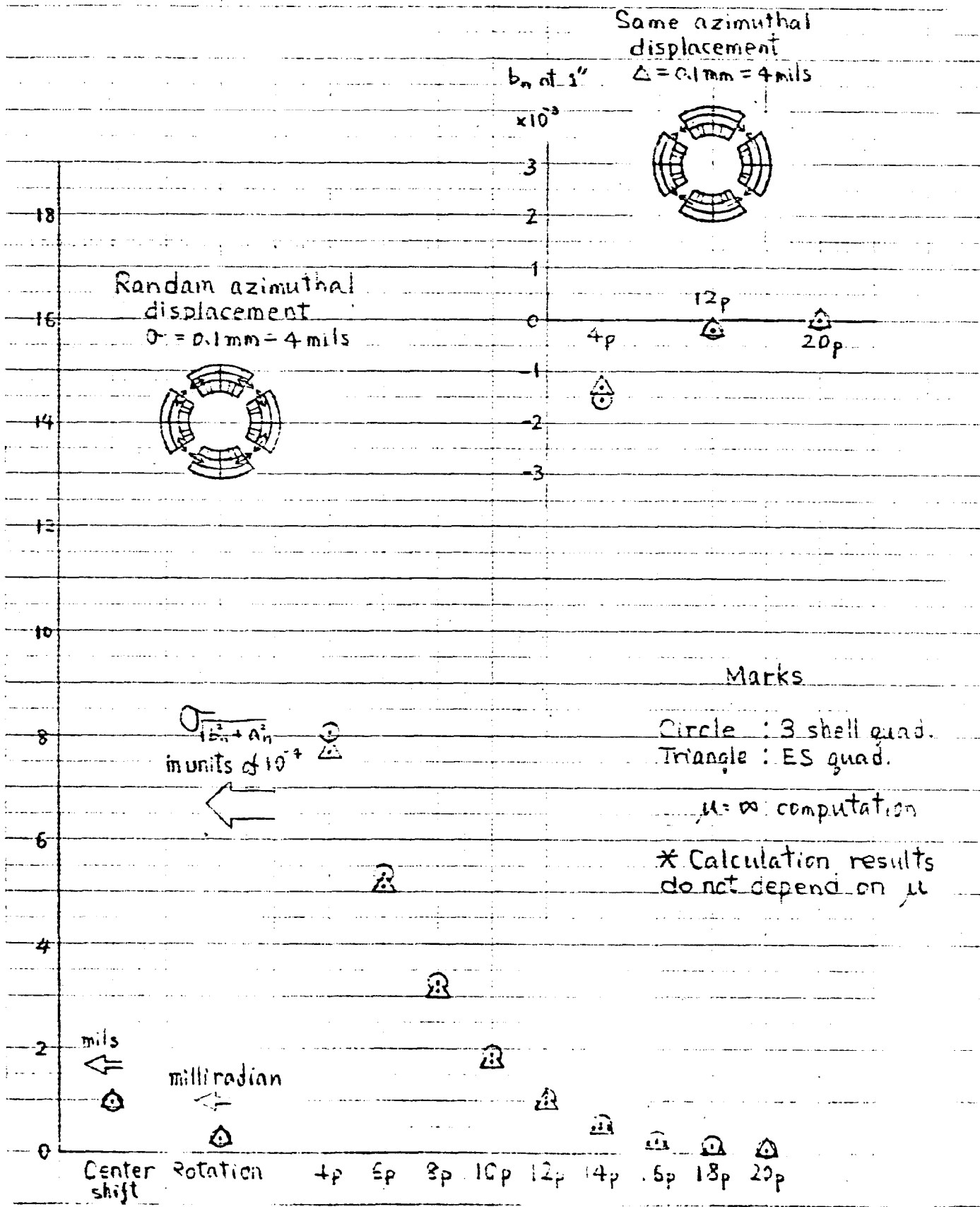


Figure 4 Harmonics variation for azimuthal displacement

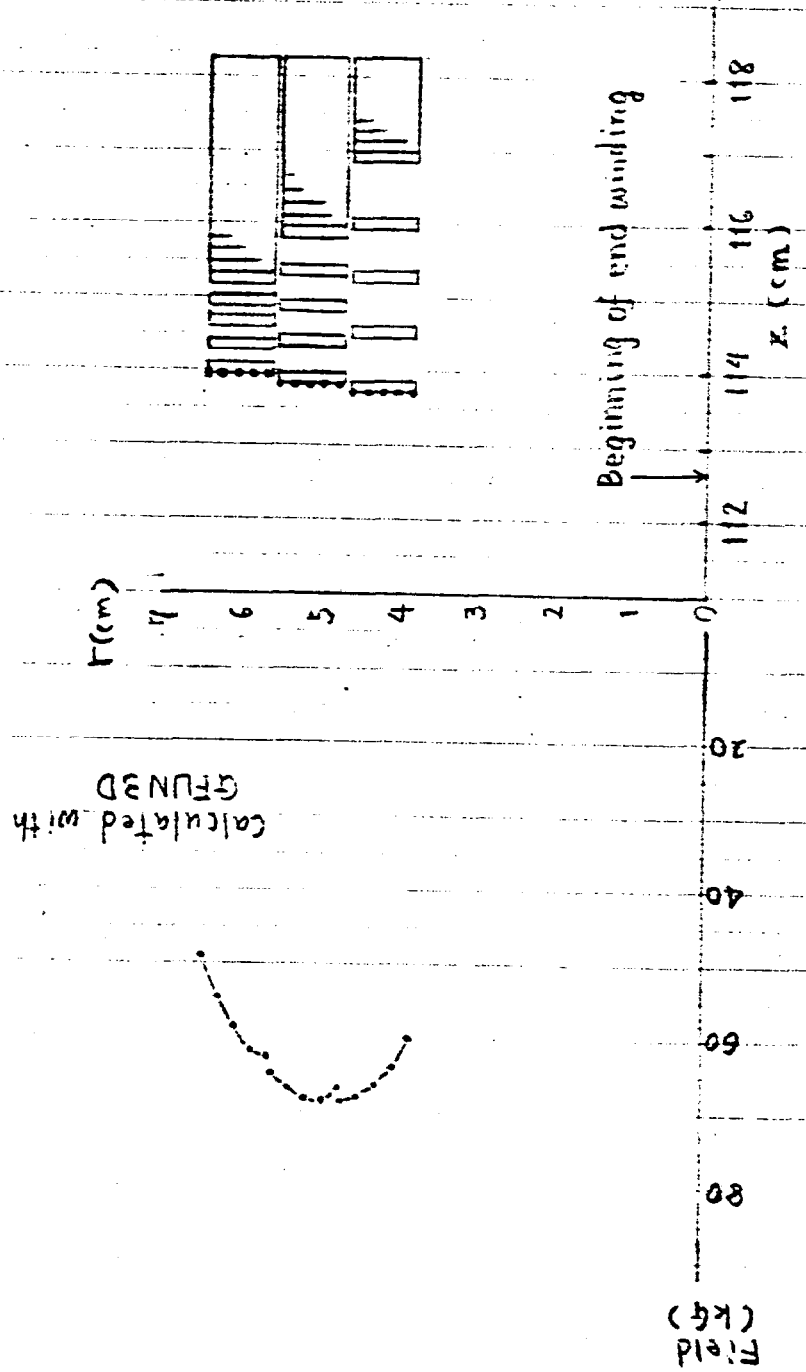
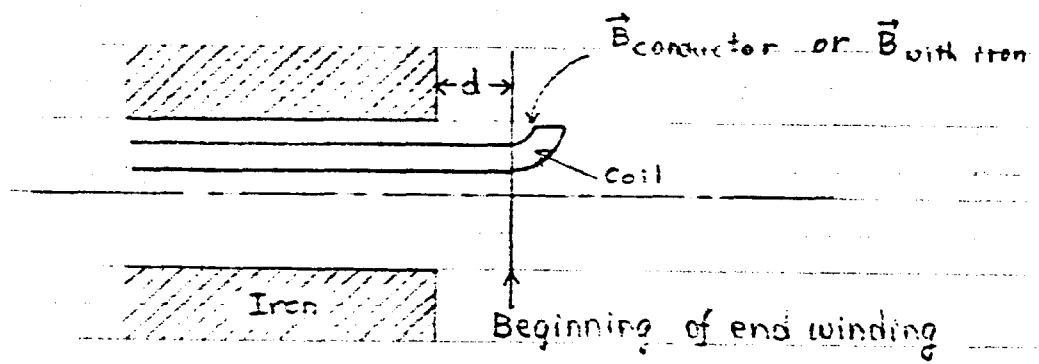


Figure 5 Magnet end winding



Field enhancement on the symmetric plane

ΔB (kG)

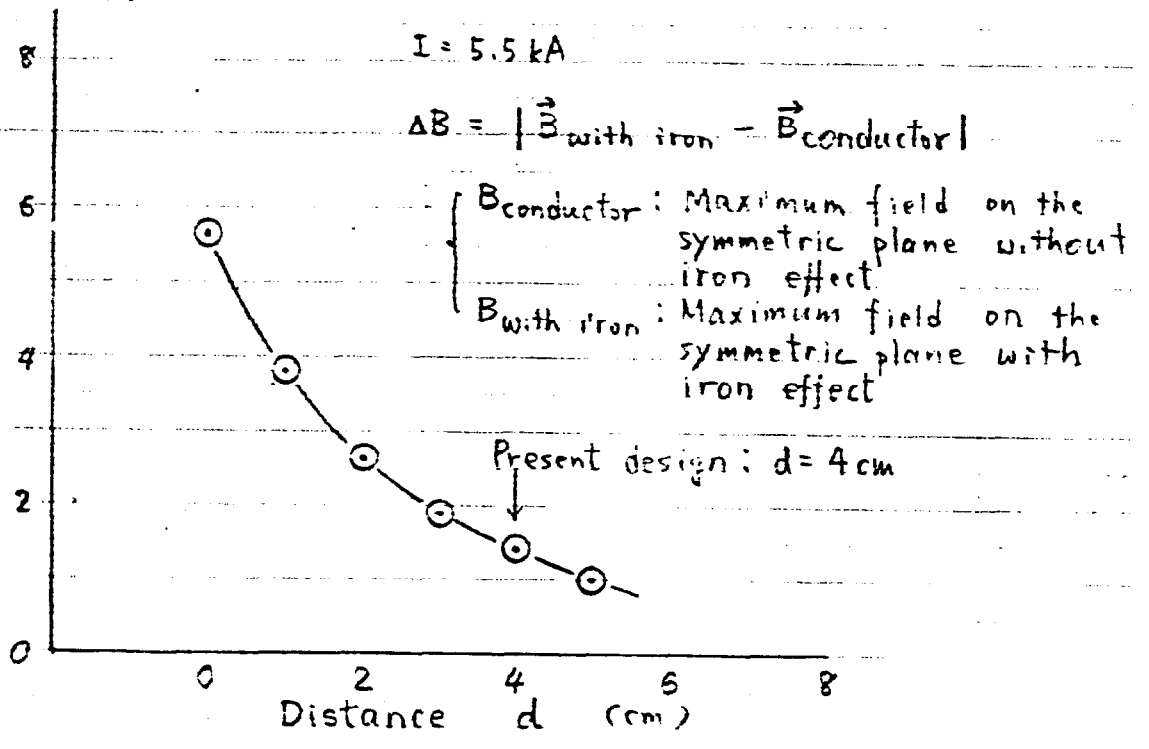


Figure 5. Iron magnetization effect at magnet edge

Strands/cable : 25
 Current : 5.6 kA
 Field gradient : 5.0 T/in

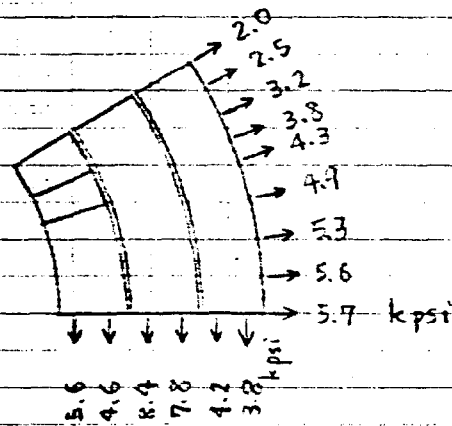


Figure 7. Magnetic pressure on the windings.

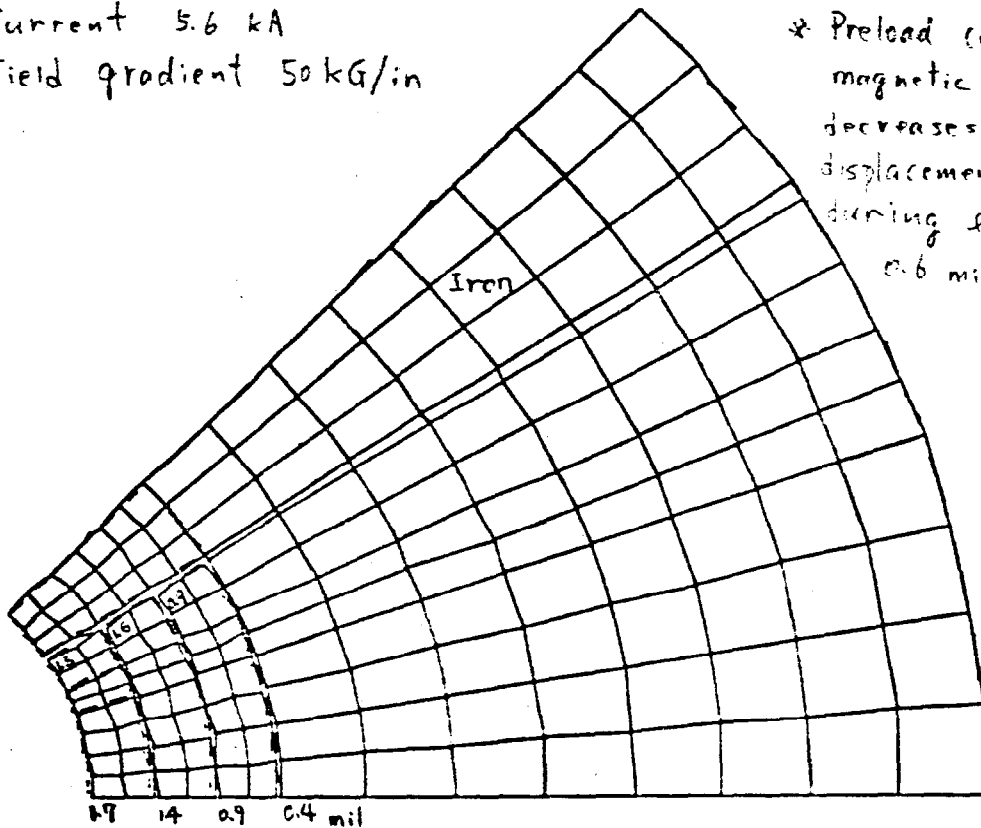
STEP= 1 ITER= 20 TIME= .00

.05000

Two-dimension calculation
No preload

Current 5.6 kA
Field gradient 50 kG/in

* Preload corresponding to the magnetic force at 50 kG/in, decreases the maximum displacement in the windings during excitation to 0.6 mil (from 1.6 mils)



DISP ANSYS 2

Figure 8. Displacement of the windings

- A: Boundary condition from symmetry
- B: Periodic boundary condition along 'z' axis
- C: Contact

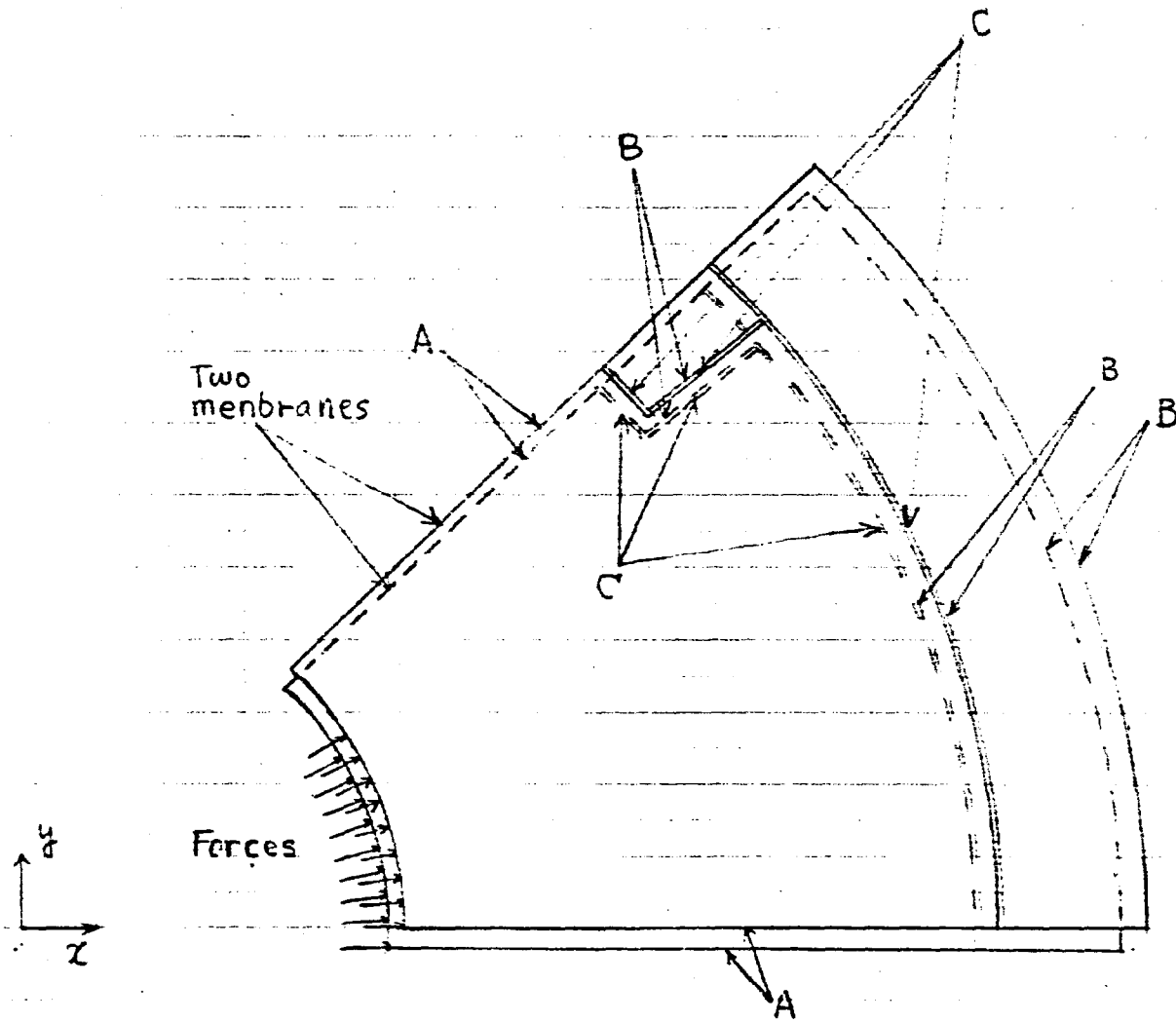


Figure 9 Boundary conditions

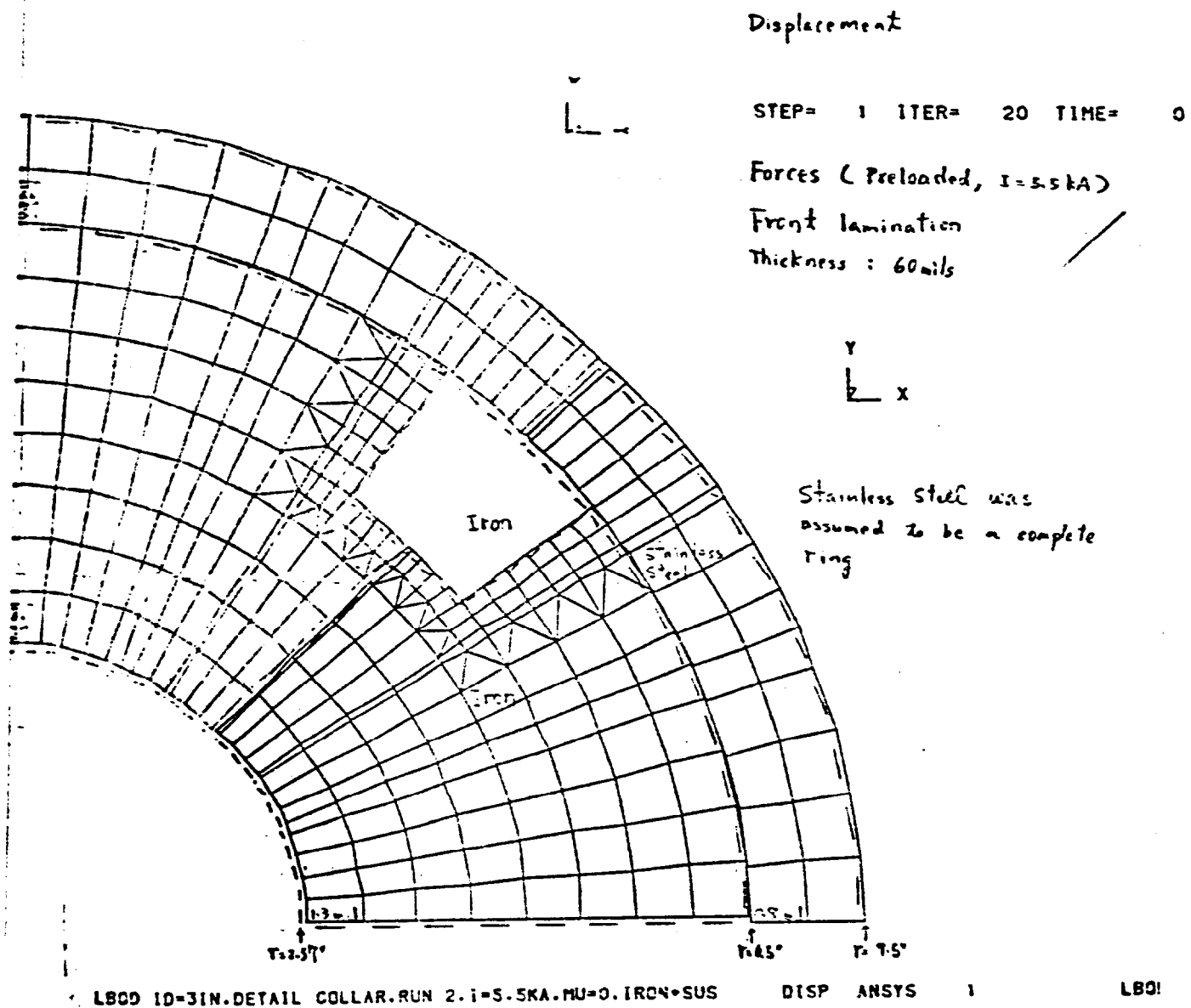
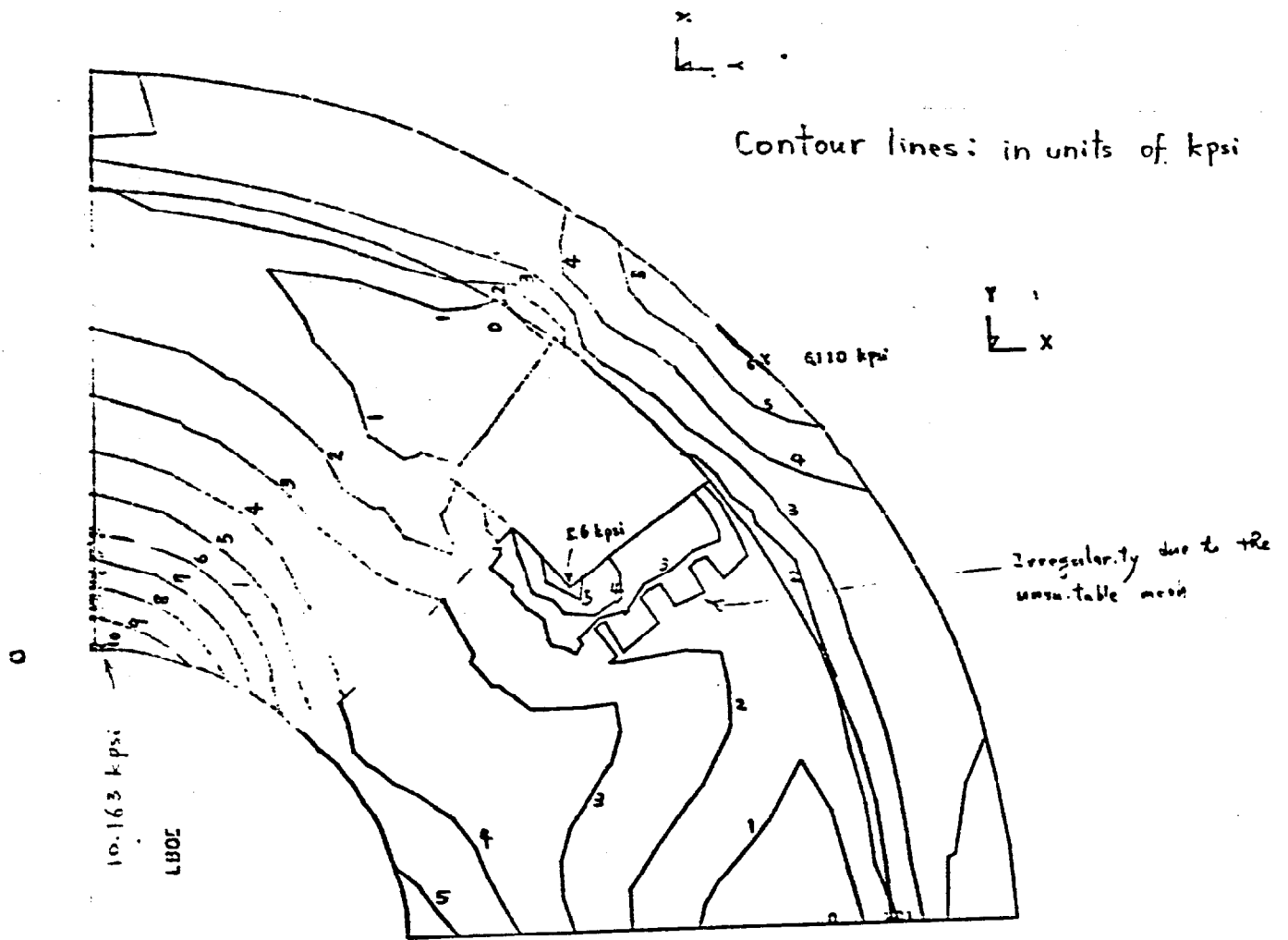


Figure 10. Deflection of the collar



09 ID=3IN-DETAIL COLLAR.RUN 2.1-5.SKA.MU=0.IRON+SUS SGET ANSYS 2

Figure 11 (A). Stress on the collar

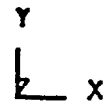
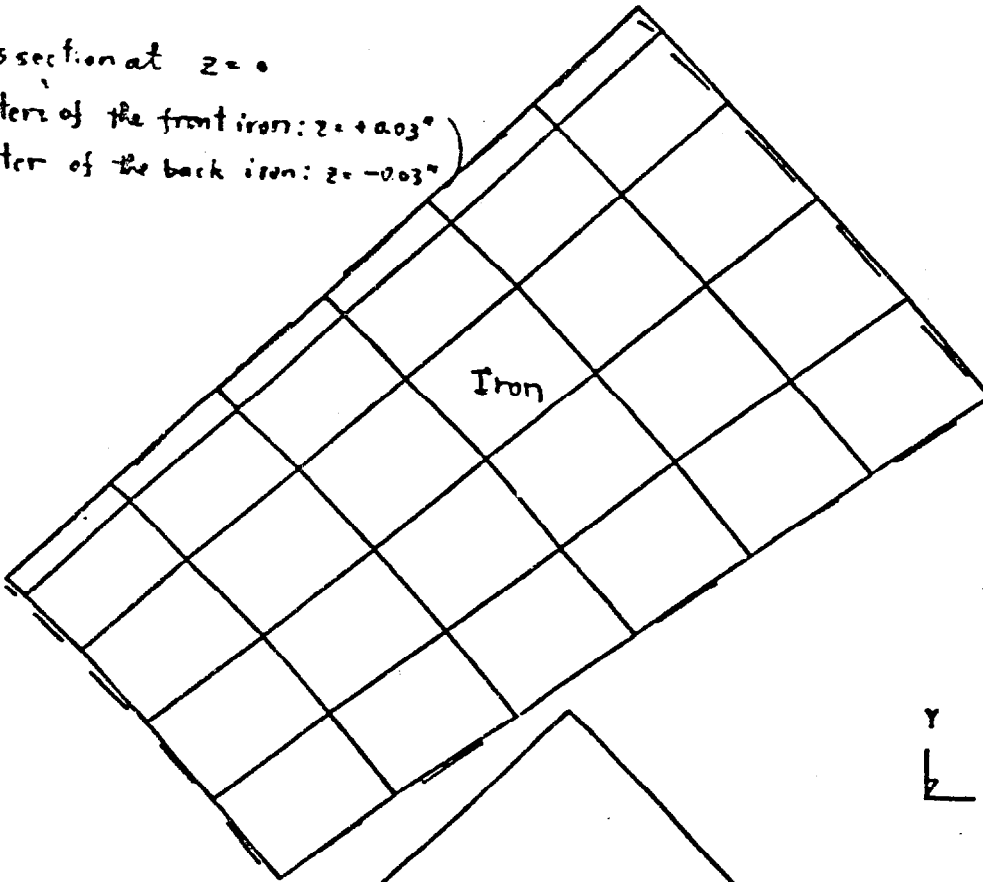
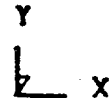
STEP= 1 ITER= 20 TIME= 0

.02000

Key

Cross section at $z = 0$

{ Centers of the front iron: $z = +0.03"$
center of the back iron: $z = -0.03"$



Contour lines in units of kpsi

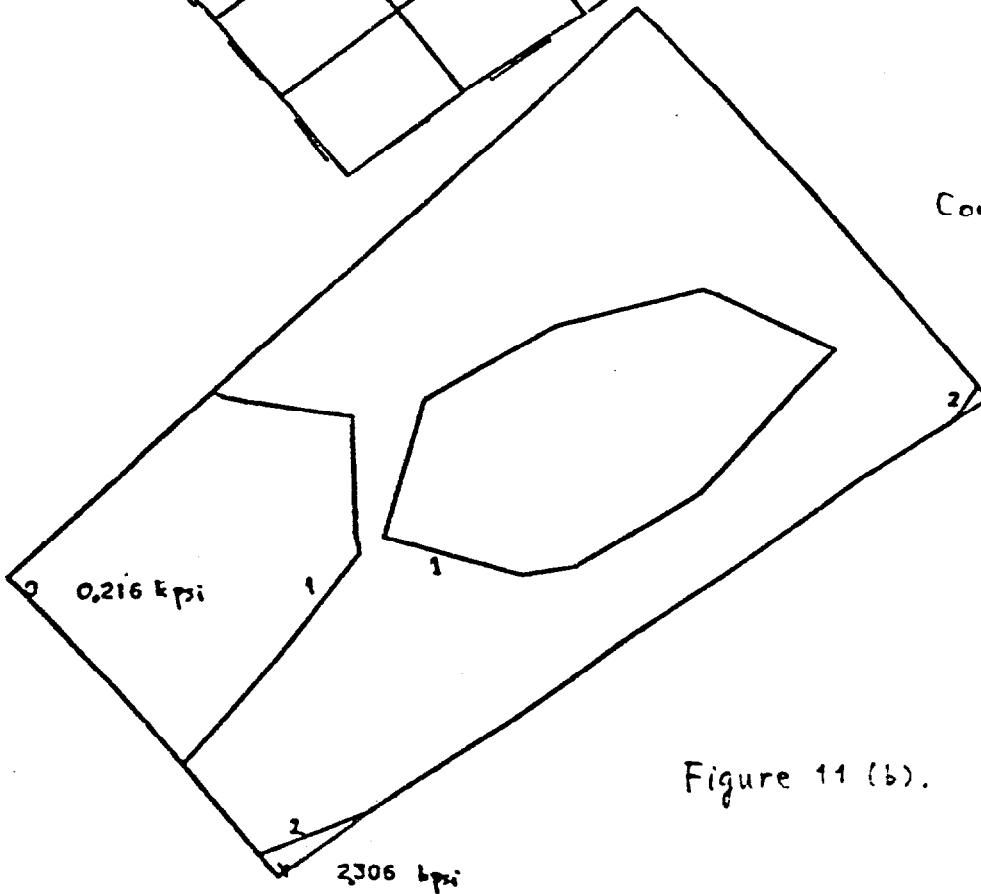


Figure 11 (b). Stress on the key